Vol. 589: 13–31, 2018
https://doi.org/10.3354/meps12420

MARINE ECOLOGY PROGRESS SERIES
Mar Ecol Prog Ser

Published February 23

Seasonal succession of phytoplankton community structure from autonomous sampling at the Australian Southern Ocean Time Series (SOTS) observatory

Ruth Eriksen[1,2,*], Thomas W. Trull[1,2], Diana Davies[1], Peter Jansen[1], Andrew T. Davidson[3], Karen Westwood[3], Rick van den Enden[3]

[1]Antarctic Climate and Ecosystems Cooperative Research Centre, Private Bag 80, Hobart, Tasmania 7001, Australia
[2]CSIRO Oceans and Atmosphere, Castray Esplanade, Battery Point, Tasmania 7004, Australia
[3]Australian Antarctic Division, 203 Channel Highway, Kingston, Tasmania 7050, Australia

ABSTRACT: Limited knowledge of phytoplankton community structure in the Southern Ocean hampers our understanding of ecosystem function and its response to changes expected this century from anthropogenic CO_2 emissions and associated climate warming. To address this gap, we obtained records of phytoplankton community composition and nutrient concentrations, collected at 9-d intervals over the austral production season from September 2010 to April 2011 at the Southern Ocean Time Series observatory (46° 56′ S, 142° 15′ E) using an autonomous sampler, accompanied by hourly sensor-based estimates of water column structure and light levels. Satellite ocean colour and *in situ* fluorescence showed a moderate increase in phytoplankton biomass, 4–5 fold, from winter to mid-summer. Total cell number and biovolume increases were larger (up to 80-fold and 40-fold, respectively), reflecting the importance of heterotrophs and smaller organisms. The haptophyte *Phaeocystis antarctica* dominated abundances (up to 75%), but only constituted a few percent of total biovolume, which was dominated by diatoms and dinoflagellates. Ciliates contributed less than 5% of abundance, while tintinnids were rarer still. Community analysis of species similarities identified 3 distinct clusters, tracking seasonal shallowing of the mixed layer (from 500 to 50 m) and decreased silicate availability (from ~4 to <1 µM). The diatom:dinoflagellate biovolume ratio decreased more strongly than their abundance ratio, consistent with progression towards small weakly silicified diatoms in summer. Silicoflagellates were associated with elevated winter and spring silicate levels. The overall nitrate/silicate depletion ratio was ~2, indicating significant export by the non-diatom community. Exploratory correlative analysis of the biological diversity with environmental conditions suggests mixed layer depth and silicate levels as more likely drivers than inputs from subtropical waters or biomass accumulation.

KEY WORDS: Southern Ocean Time Series · Phytoplankton · Autonomous sampler · Community structure · *Phaeocystis*

INTRODUCTION

The Southern Ocean (SO) has a significant influence on marine biogeochemistry globally. It is responsible for the supply of oxygen to the deep ocean interior (Matear et al. 2000), upwelling of nutrients that fuel much of global surface ocean productivity (Sarmiento et al. 2004), and regulation of climate from decadal to interglacial time scales through sequestration and release of CO_2 (Sarmiento & Le Quéré 1996, Sigman & Boyle 2000). Plankton strongly influences these cycles, because it is the balance between upwelled supply of CO_2 and local biological consumption of nutrients that determines the net

*Corresponding author: ruth.eriksen@csiro.au

transfer of CO_2 to the atmosphere, the export of particulate carbon to the interior, and the amount of residual nutrients available for transport to the rest of the ocean (Trull et al. 2001a, Takao et al. 2014, Shadwick et al. 2015). Efficiency of these biological processes in the SO is controlled by iron, limiting primary productivity, influencing floristic composition, and resulting in the largest high-nutrient low-chlorophyll (HNLC) region in the global ocean (Martin 1990, de Baar et al. 1995, Banse 1996, Blain et al. 2007). The Subantarctic Zone (SAZ) represents approximately half of the area of the SO, and is the location of the formation of mode and intermediate waters that are responsible for significant sequestration of anthropogenic CO_2 (Sabine et al. 2004). The SAZ is the interface between the SO and waters further north, and exhibits seasonal changes that range from fully macronutrient replete in winter to significant depletion in summer, especially for silicates (Dugdale et al. 1995, Trull et al. 2001b). The SAZ is the focus of this work.

Under future climate scenarios, predicted changes to the SO include increased temperature and higher winds with subsequent changes to stratification, light availability and nutrient resupply to the upper sunlit layer (Matear & Hirst 1999, Boyd et al. 2008, Deppeler & Davidson 2017). Increased zooplankton grazing of phytoplankton may also ensue from their greater sensitivity to climate warming (e.g. Laws 2004, Behrenfeld 2014), or changing phenology and distribution of zooplankton grazers (Poloczanska et al. 2016). Examining seasonal community changes may eventually help to inform the identification of the relative importance of nutrients, carbon system properties, temperature, light, mixing, and grazing on community composition in the SO; these are key issues in the projection of responses to climate change (Boyd & Doney 2002, 2003, Boyd et al. 2008). Possible influences on seasonal phytoplankton dynamics have long focused on nutrient supply and turbulence or mixing as major factors (Margalef 1978). Recently, there has been growing emphasis on trace metals, pH and CO_2 concentrations as important influences (Strzepek et al. 2012). Grazing regimes (top-down controls) may also modulate accumulation of biomass, species composition and phytoplankton size structure in the SO (Legendre & Le Fevre 1995, Turner 2015).

The SAZ of the SO supports a diverse phytoplankton community (Kopczynska et al. 2007, de Salas et al. 2011, Cassar et al. 2015); however, little is known about the seasonal structure and evolution of phytoplankton communities despite their importance in developing and refining models of ecosystem function (Arrigo et al. 1999, Queguiner 2013, Takao et al. 2014). Diatom species, for example, have varying seasonal life strategies and respond differently to iron and silica availability (Cortese & Gersonde 2007, Marchetti & Cassar 2009, Queguiner 2013). Some phytoplankton species contribute more to carbon export than others (Assmy et al. 2013), influenced by their morphology or mucous formation on particle aggregation and sinking rates (Schoemann et al. 2005, Laurenceau-Cornec et al. 2015), while the response of coccolithophores to warming and acidification appears to be strain specific (Cubillos et al. 2007). The specifics of species interactions with zooplankton are similarly complex and influence seasonal cycles (Morel et al. 1991, Strom et al. 2003) and export (Legendre & Le Fevre 1995, Schoemann et al. 2005, Ebersbach et al. 2011, Turner 2015). Thus, detailed study of the seasonal changes in community composition to as deep a level of taxonomic identification as possible is warranted.

The scale and remoteness of the SAZ hampers *in situ* studies of phytoplankton, with investigations typically consisting of intensive, short-term, and spatially restricted process studies (Bowie et al. 2011, de Salas et al. 2011), or sparsely sampled transects across large areas of ocean with associated variations in hydrographic and biological controls, sometimes repeated for multiple years (Kopczynska et al. 2007, Wright et al. 2010, Takao et al. 2014). Each of these approaches provides important information on community composition, but cannot capture the detailed seasonality of physical and chemical controls, or species responses. To address this gap, the Southern Ocean Time Series (SOTS) program deploys an autonomous water sampler in the SAZ mixed layer, allowing high-resolution sensor data to be coupled with discrete water samples preserved *in situ*, for analysis once the package is retrieved (Trull et al. 2010, Weeding & Trull 2014, Shadwick et al. 2015). In this study, we collected paired samples every 9 d from early spring 2010 to late autumn 2011 for nutrient analysis and phytoplankton identification. The frequency of sampling and the duration of the deployment allowed a number of questions about phytoplankton community dynamics in the SAZ to be explored: (1) what is the composition of the phytoplankton community in the SAZ; (2) how does this community vary seasonally; and (3) how are the variations influenced by environmental conditions?

This paper presents the first autonomous record of seasonal community structure in the SAZ, and briefly explores its relationships to environmental condi-

tions. Future efforts from ongoing deployments will determine its representativeness and then work to address the larger issues of potential future changes in SO ecosystems, including the role of phytoplankton in the biogeochemical pump, and the cycling of silica and carbon.

MATERIALS AND METHODS

Overview of the SOTS observatory

The SOTS observatory is a facility of the Australian Integrated Marine Observing System (IMOS) consisting of 3 deep ocean moorings: the Southern Ocean Flux Station (SOFS), the SAZ sediment trap mooring, and the Pulse Biogeochemistry mooring. The Pulse mooring design addresses challenges associated with collecting measurements from the surface mixed layer, in a deep (>4000 m) site with rough bathymetry and notoriously severe sea-state conditions (Pender et al. 2010). The mixed-layer instrument and water sampler package is suspended from a small surface float at 32 m depth using elastic links to decouple it from surface wave stresses. Locating the SOTS site in the SAZ is based on (i) the rarity of sustained observations in the SO, (ii) existing and ongoing supporting observational programs such as the World Ocean Circulation Experiment (WOCE) and Ships of Opportunity programs, (iii) previous detailed ship-based process studies, and (iv) capacity to be serviced by research and Antarctic resupply vessels based in Hobart, Tasmania. Comparison to satellite and *in situ* oceanographic observations suggest it is representative of a broad longitudinal swath of the HNLC SAZ from ~90 to 145° E (Trull et al. 2010, Shadwick et al. 2015).

Oceanographic characteristics of the SOTS site

The SOTS Pulse mooring lies to the south of the Subtropical Front (STF), approximately 530 km southwest of Tasmania at 46° 56′ S, 142° 15′ E (Fig. 1A). The oceanography and biogeochemistry of the region are well characterized from multiple repeats of WOCE/CLIVAR SR3 hydrographic sections and 'MV L'Astrolabe' Antarctic resupply transits (Rintoul et al. 1997, Rintoul & Bullister 1999, Sokolov & Rintoul 2002, Bender et al. 2016), dedicated process

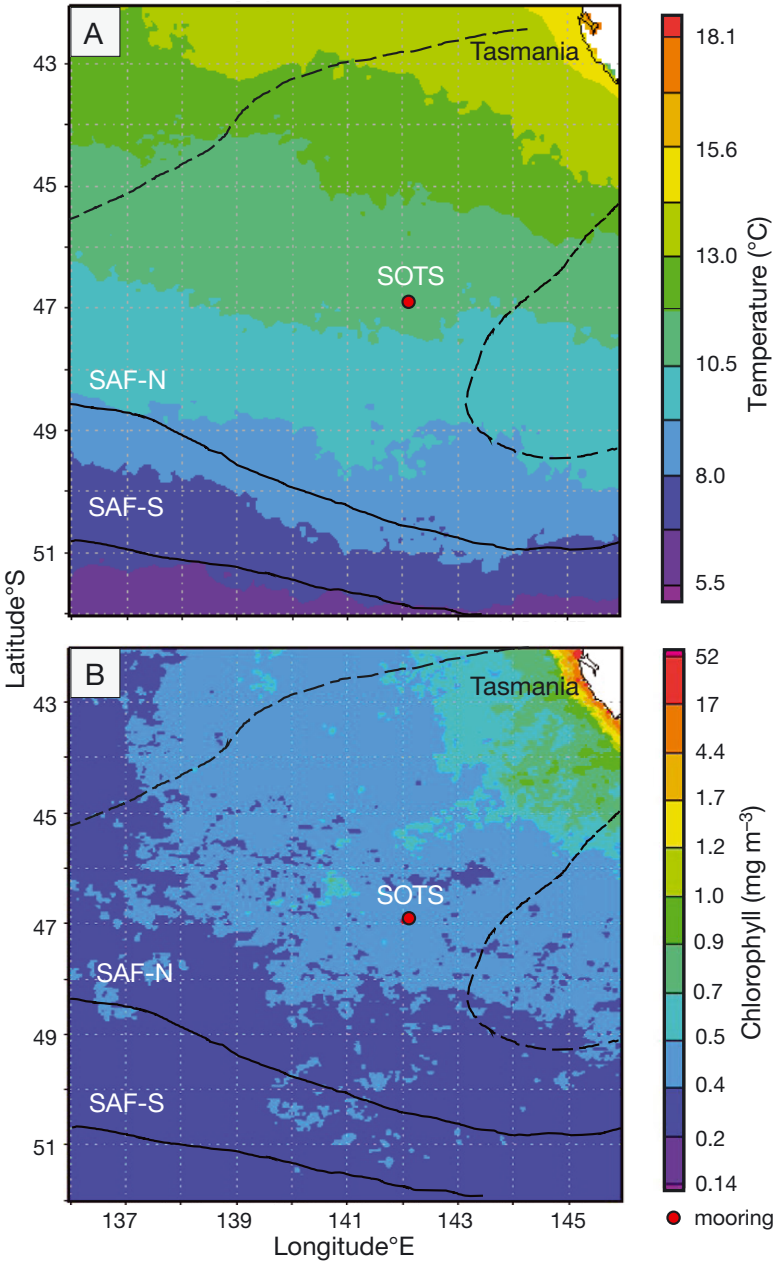

Fig. 1. Location of the Southern Ocean Time Series (SOTS) observatory and (A) average satellite sea surface temperature (°C) and (B) average chlorophyll (MODIS Aqua, mg m^{-3}) for the deployment period. Solid lines indicate locations of the north and south branches of the Subantarctic Front (SAF-N and SAF-S) derived from Sokolov & Rintoul (2002). Dashed line indicates maximum gradient of sea surface height in the Sub Antarctic Zone, as per Herraiz-Borreguero & Rintoul (2011)

studies (Trull et al. 2001c, Bowie et al. 2011, Cassar et al. 2015), and mooring-based observations that began with deep-ocean sediment traps in 1997 (Trull et al. 2001a) and are ongoing as part of the SOTS (e.g. Weeding & Trull 2014, Shadwick et al. 2015, present study). The SOTS site is representative of conditions for a large proportion of the Indian and Australian sectors of the SAZ (Trull et al. 2001a), and lies within a weak anti-cyclonic gyre with predominantly westward flow (Herraiz-Borreguero & Rintoul 2011).

The seasonal cycle of mixed-layer depth (MLD) is extreme, reaching more than 500 m in late winter and remaining relatively deep (>50 m) through summer (Rintoul & Trull 2001). Seasonal warming is relatively small at ~3.5°C. Phosphate and nitrate are abundant all year, but silica is depleted by late summer (Bowie et al. 2011). Iron limits primary production (Sedwick et al. 1999, 2008) and, along with grazing, keeps phytoplankton biomass accumulation small (typically less than 0.6 µg chlorophyll l^{-1}). This results in a moderate biologically driven sink for atmospheric CO_2 with subdued seasonality (Shadwick et al. 2015). Annual net community production is difficult to determine because of large exchanges between the surface mixed layer and underlying waters, but appears to be moderate at ~2 moles O_2 m^{-2} (Weeding & Trull 2014), delivering organic carbon to the ocean interior at rates close to the global median (~1 g particulate organic carbon m^{-2} yr^{-1} at 1000 m depth) in association with calcium carbonate as the dominant mineral phase (Trull et al. 2001a). As summarized in 'Results', water column conditions in the 2010–2011 austral season were very similar to these previous results.

Seawater sample collection

A Remote Access Sampler (RAS-500 McLane Labs) filled forty-eight 500 ml Tedlar bags in pairs (collected 1 h apart at 02:00 and 03:00 UTC) at preprogrammed 9-d intervals, between 12 September 2010 and 7 April 2011 (Table S1 in the Supplement at www.int-res.com/articles/suppl/m589p013_supp.pdf).

The RAS uses a common inlet and distributes samples to the bags via a multi-port valve without passing through a pump, thus avoiding mechanical damage of cells and potential contamination from pump components. The smallest cross-sectional area of the sampling flow path is 1.51 mm^2 (diameter 1.39 mm) and thus should effectively sample all phytoplankton species, including colonial and chain-forming morphologies. A black plastic shroud and a 1000 µm plastic mesh shield on the sample inlet were added to minimize bio-fouling of the sampler and inlet (Pender et al. 2010). In between collection events, the sample inlet was back-flushed with mercuric chloride biocide (500 µM) to prevent biological growth.

Prior to deployment, the RAS was primed with approximately 5 ml of distilled, deionized water, filling all spaces to prevent air-locks. One bag in each pair was pre-loaded with saturated aqueous mercuric chloride (Alfa Aesar Puratronic, 99.999%, to achieve a final concentration of 80 µM in the collected sample) for measurement of dissolved constituents (without filtration), including inorganic carbon, alkalinity and nutrients. The other bag in each pair was pre-loaded with microscopy-grade, low-acidity glutaraldehyde (Merck, final concentration 1%).

Protist identification

Upon retrieval, samples were refrigerated at 4°C in the dark until analysis. Due to the biomass, samples were pre-concentrated by sedimentation. Sample bags were gently mixed, and the entire sample volume was decanted into 500 ml tall-form measuring cylinders, and Lugols iodine was added to aid sedimentation (Sournia 1978). The settled samples were drawn down to 100 ml after 1 wk, decanted into tall-form 100 ml cylinders and concentrated to a final volume of 15 ml after a further 1 wk of settling. Pre-concentrated samples were stored in amber glass vials at 4°C until examination. Counts were performed on a 6 ml aliquot transferred to a Utermöhl chamber, using an Olympus IX81 inverted microscope (differential interference contrast or phase contrast) at 320×. The highest magnification for identification was 630×. The entire chamber was scanned for species composition, and consecutive fields of view were examined until 400 cells of the dominant group or species were observed (typically *Phaeocystis*). Counts (as cells l^{-1}) were corrected for the proportion of the chamber counted and the concentration factor. The limits of light microscopy mean that nanoplankton (2–20 µm), microplankton (20–200 µm), and smaller members of the mesoplankton (200–2000 µm) are the focus of the observations described here. Unless possessing distinctive morphology, cells <5 µm were collectively grouped as URGOs (unidentified round green objects), and will be the subject of more detailed examination by electron microscopy in future work.

Primary references for phytoplankton identification were Hallegraeff et al. (2010), Scott & Marchant (2005), Tomas (1997) and references therein. Primary

references for loricate ciliates were Dolan et al. (2012) and Petz (2005) (in Scott & Marchant 2005) and Petz (1999). Data were grouped into major taxonomic or morphological groups: diatoms, dinoflagellates, flagellates, silicoflagellates, ciliates (naked and loricate), and a final 'other' category for unidentified cells and rarer materials such as pollen, appendicularians, and foraminiferans. All cells were binned into size classes for biovolume calculation ($\mu m^3\ l^{-1}$) as per Hillebrand et al. (1999), Cornet-Barthaux et al. (2007), Leblanc et al. (2012), and de Salas et al. (2011), noting that preservatives may affect cell size, causing either shrinkage or swelling (Menden-Deuer et al. 2001), potentially affecting both biovolume estimates and conversion to carbon biomass. For tintinnids, mechanical disturbance and fixation often provokes detachment of the cell and, therefore, we did not differentiate between live and empty tintinnid loricae (Thompson et al. 1999). Images of preserved cells from a range of taxonomic groups are included in the Supplement (see Fig. S1). Estimation of the degree of silicification for diatom species is based on microscopic examination, and the taxonomic literature.

Data for phytoplankton community composition have been archived in the Australian Phytoplankton Database (Davies et al. 2016). Both abundance and biovolume data are available for download from the Australian Ocean Data Network (AODN) portal (https://portal.aodn.org.au/). The data may be found by searching AODN for the Australian Phytoplankton Database, and selecting the project name 'Southern Ocean Time Series' (IMOS dataset number P805).

Ancillary measurements

Sensors recorded temperature and salinity (Seabird SBE16+V2 CTD), photosynthetically active radiation (PAR) (Alec Electronics), chlorophyll fluorescence and red light back-scatter (Wetlabs FLNTUS instrument with an anti-biofouling wiper), dissolved oxygen (Aanderaa optode 3835 and Seabird SBE-43 electrode), and total dissolved gases (Pro-oceanus Gas Tension Device). Instruments were calibrated at the CSIRO Calibrations Facility (Hobart, Tasmania) and Sea Bird Electronics, and serviced before and after deployment. Detailed analysis of the temperature, salinity, MLD, oxygen and gas tension measurements for the Pulse-7 deployment were presented in Weeding & Trull (2014).

Conversion of the FLNTUS fluorescence record to chlorophyll was based on the manufacturer's calibration (uranine working standards with normalisation to a 25 $\mu g\ l^{-1}$ chlorophyll *a* suspension of *Skeletonema costatum* diatom cells; Wetlabs), owing to a lack of *in situ* pigment measurements for this deployment of the Pulse package. This lack of local calibration means that the conversion of chlorophyll fluorescence to concentration is quite uncertain. Roesler et al. (2017) showed that the manufacturer's calibration of fluorescence instruments significantly overestimates SO chlorophyll concentrations by 5- to 8-fold (versus pigment samples), and their comparison of radiometric and fluorescence chlorophyll estimates on autonomous profiling floats suggests 3.5- to 4.5-fold for our South Indian sector. Accordingly, we display our fluorescence results divided by a factor of 4. This brings them into reasonable accord with the MODIS satellite remote sensing chlorophyll estimates (after their adjustment for improved regional calibration against *in situ* pigment measurements, as described below). We also removed fluorescence data from mid-December onward when it became very noisy and elevated and the FLNTUS backscatter instrument showed large spikes, suggesting biofouling (data not shown).

The daily average levels of PAR available to support photosynthesis were estimated from the Alec Electronics sensor hourly in-air records from the Pulse surface float, assuming 98% transmission across the air–water interface and a blue-water attenuation length scale of 25 m (Kirk 1994). This attenuation length choice was consistent with a ship CTD PAR profile obtained in August 2011 (23.3 m, voyage IN2011_V03 CTD 21, data not shown), and provides an upper limit to PAR availability, given that biomass accumulation reduces the attenuation length scale (e.g. to 13.5 m in March; based on ship CTD PAR profiles). Importantly, our Alec PAR sensor has not been through rigorous calibration, and we scaled the results by dividing by a factor of 5 to bring them into accord with results from the ship CTD. This scaling is approximate, and the PAR estimates should be considered approximate, probably not better than a factor of 2. Fortunately, this large uncertainty does not compromise the main PAR results as used in our interpretation below, that PAR availability is controlled by MLD and varies between growth limiting low levels in winter and moderate levels without photo-inhibition in summer, consistent with previous results in this region (Westwood et al. 2011).

Dissolved nutrients (silicate, phosphate, and the sum of nitrite+nitrate, hereafter referred to simply as nitrate) were measured on the mercuric chloride preserved, unfiltered samples at CSIRO Marine Labora-

tories (Hobart, Tasmania) using Lachat QuickChem spectrophotometric methods 31-115-01-1-I, 31-107-04-1-A, and 31-114-27-1-D. Detection limits were 0.02 µM P, 0.05 µM N, and 0.1 µM Si, and data were corrected for dilution by the prime volume, based on comparing measured sample and *in situ* (RAS package CTD) salinities. The seasonal cycle of nutrient concentrations determined using these samples is very similar to that based on CTD Niskin samples (Lourey & Trull 2001), and on this basis we consider the RAS sampling technique to be free of biases.

Satellite sea-surface temperature and chlorophyll visualisations were produced with the Giovanni online data system, developed and maintained by the NASA GES DISC. Due to extensive cloud cover, MODIS-Aqua surface chlorophyll images for selected dates only, and the average for the whole deployment period are presented. Johnson et al. (2013) showed this chlorophyll product underestimates *in situ* chlorophyll levels south of Australia by a factor of 1.74 (mode of 95% range from 0.4 to 4), and for the purposes of comparison to our *in situ* FLNTUS instrument fluorescence based chlorophyll estimates, we increased the MODIS values by this factor.

Multivariate analyses

Exploratory multivariate analysis of community diversity, patterns and relationships with environmental variables were undertaken using PRIMER version 6 (Clarke & Gorley 2006). Environmental variables were normalized (by their standard deviations), and ordinations based on similarity matrices were constructed using Euclidean distance. Species abundances (cells l^{-1}) were 4th-root transformed to adjust the importance of species dominance, and the Bray-Curtis coefficient was used to calculate the resemblance matrix of between-sample similarities (Clarke & Ainsworth 1993). Ordination was by non-metric multi-dimensional scaling (nMDS), with data presented as rank order in 2D space (Clarke 1993). Hierarchical CLUSTER analysis with group average linking was also used to visualize groupings of samples over the deployment. Analysis of similarities (ANOSIM) was used to test the null hypothesis that there was no significant difference in community composition between pre-defined groups based on MLD status (deep, stratifying, shallow/stable). The SIMPER routine was used to determine which species are typical of the groups identified by CLUSTER and MDS analysis. SIMPER measures the contribution of each species to the observed average similarity within groups (verified using the ANOSIM routine) using the Bray-Curtis measure of similarity, and a cumulative cut-off of 50% (Clarke 1993). The total number of individuals (N) and number of taxa (*S*, based on abundances) are also presented.

To explore the possible role of environmental conditions on the community diversity we used the BEST routine to test for high rank correlations between the species assemblage similarity matrix and similarity matrices for different sub-sets of the environmental variables (Clarke & Ainsworth 1993). Specifically, we evaluated rank correlations with single, double, and triple variable sub-sets of our 8 environmental variables: MLD, temperature, salinity, total chlorophyll, PAR averaged over the MLD (PAR_{MLD}), and silicate, nitrate, and phosphate concentrations. As discussed below, several of these variables are strongly correlated with each other (see Table 3); thus, evaluating the rank correlations requires consideration of magnitudes of the variable changes and mechanisms of possible impact on community structure.

RESULTS

Environmental conditions during the deployment period

Surface chlorophyll estimated from MODIS satellite ocean colour was low, averaging 0.5 mg m^{-3} across the whole deployment period (Fig. 1B, noting that these values have been corrected as per Johnson et al. 2013; see 'Materials and methods'). Despite persistent cloud cover, satellite imagery revealed the seasonal development of a phytoplankton bloom to the north that extended towards the SOTS location (Fig. 2), consistent with previous evaluations of regional biomass distributions (Bowie et al. 2011). Our *in situ* fluorometer revealed similar seasonality (Fig. 3E). Low winter levels increased ~3-fold by November as stratification progressed, reaching an overall ~5-fold increase by December as stratification stabilized.

MLD estimated from the Pulse mooring (Fig. 3A) was >500 m at the end of winter and shoaled to <100 m during October. Between mid-November and mid-February, the MLD further stratified to 50–60 m. Two short-term increases to >300 m occurred in late February and early March, before a steady deepening at the end of summer and beginning of autumn. These MLD variations are consistent with seasonality inferred from ship voyages over many years (Rintoul & Trull 2001), and confirm that

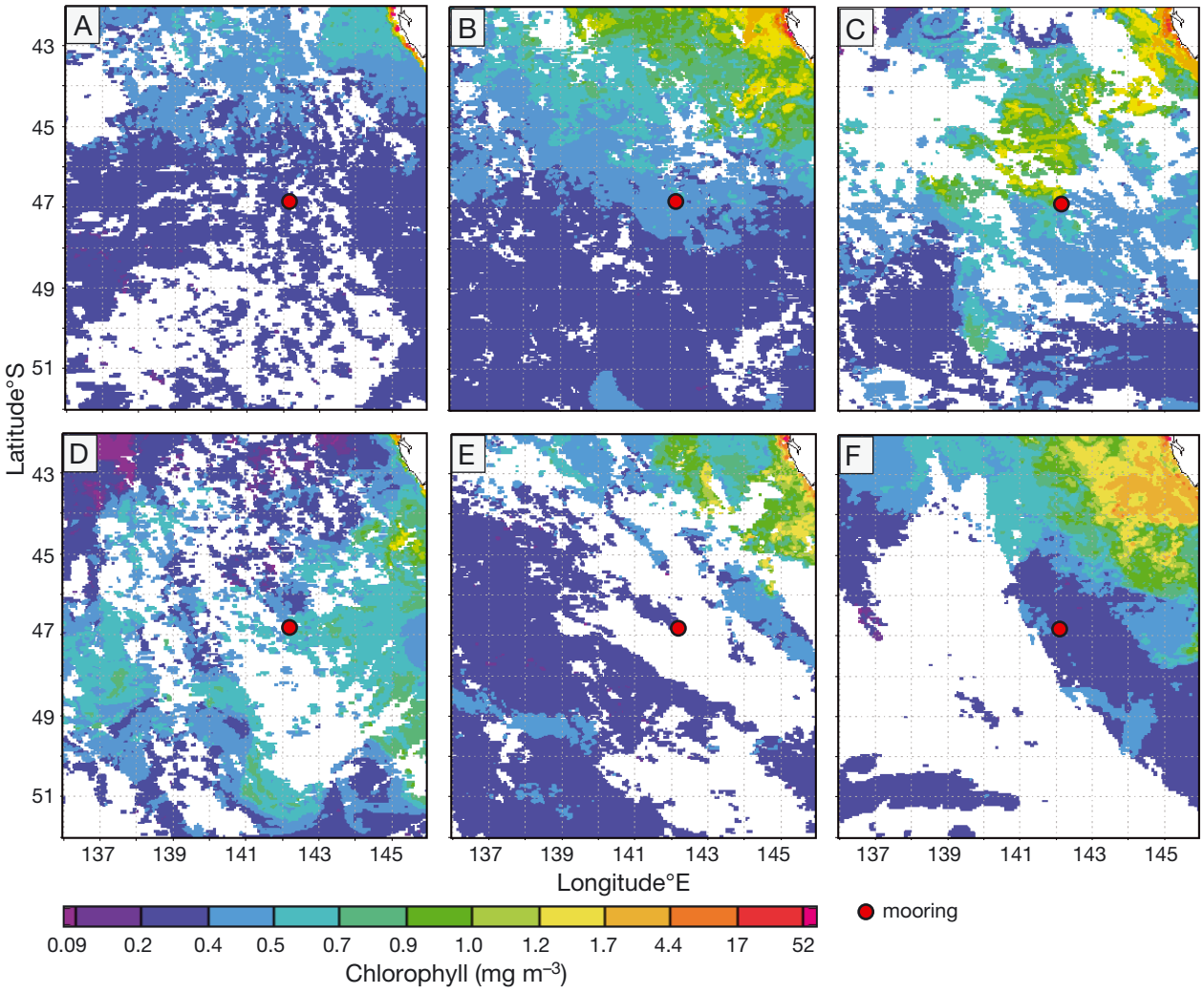

Fig. 2. Images of MODIS chlorophyll (mg m^{-3}) at selected dates during the Pulse 7 deployment, from (A) 8 October 2010, (B) 24 October 2010, (C) 25 November 2010, (D) 1 January 2011, (E) 6 March 2011 and (F) 7 April 2011. Location of Southern Ocean Time Series (SOTS) observatory is shown as a red dot

the winter MLDs in this region are deeper than the circumpolar SAZ average (~400 m) as assembled from Argo floats (Dong et al. 2008). Atmospheric pressure, wind speed, and wave strengths for this deployment were discussed in detail in Weeding & Trull (2014) and showed no discernible seasonal pattern. Water temperature ranged from 8.6°C in late winter to a summer maximum of 12.1°C, consistent with the long-term average total seasonal amplitude of 3.5°C for the SAZ south of Australia (Trull et al. 2001b).

Salinity gradually increased by 0.25 (from 34.53 to 34.78) as summer progressed, and was marked by the passage of distinctly saltier water parcels derived from modified subtropical waters in November 2010 (Fig. 3C). The seasonal cycle of MLD was the dominant control on the levels of PAR (Fig. 3D) experienced by phytoplankton, with mean daily values, averaged over the mixed layer and 24-h cycle, increasing from very low (<5 µmol m^{-2} s^{-1}; i.e. <0.5 mol m^{-2} d^{-1}) in winter and early spring to moderate levels in mid-summer (~75 µmol m^{-2} s^{-1}; i.e. ~7 mol m^{-2} d^{-1}). These ranges are consistent with the classical view of temperate marine ecology that light limitation limits growth in early spring and is alleviated by stratification (Sverdrup 1953), but without reaching saturation or inducing photo-inhibition (MacIntyre et al. 2002, Westwood et al. 2011, Strzepek et al. 2012).

Nitrate, phosphate, and silicate concentrations reached maximum values in October (Fig. 3F), consistent with the SOTS results for pCO_2 that show

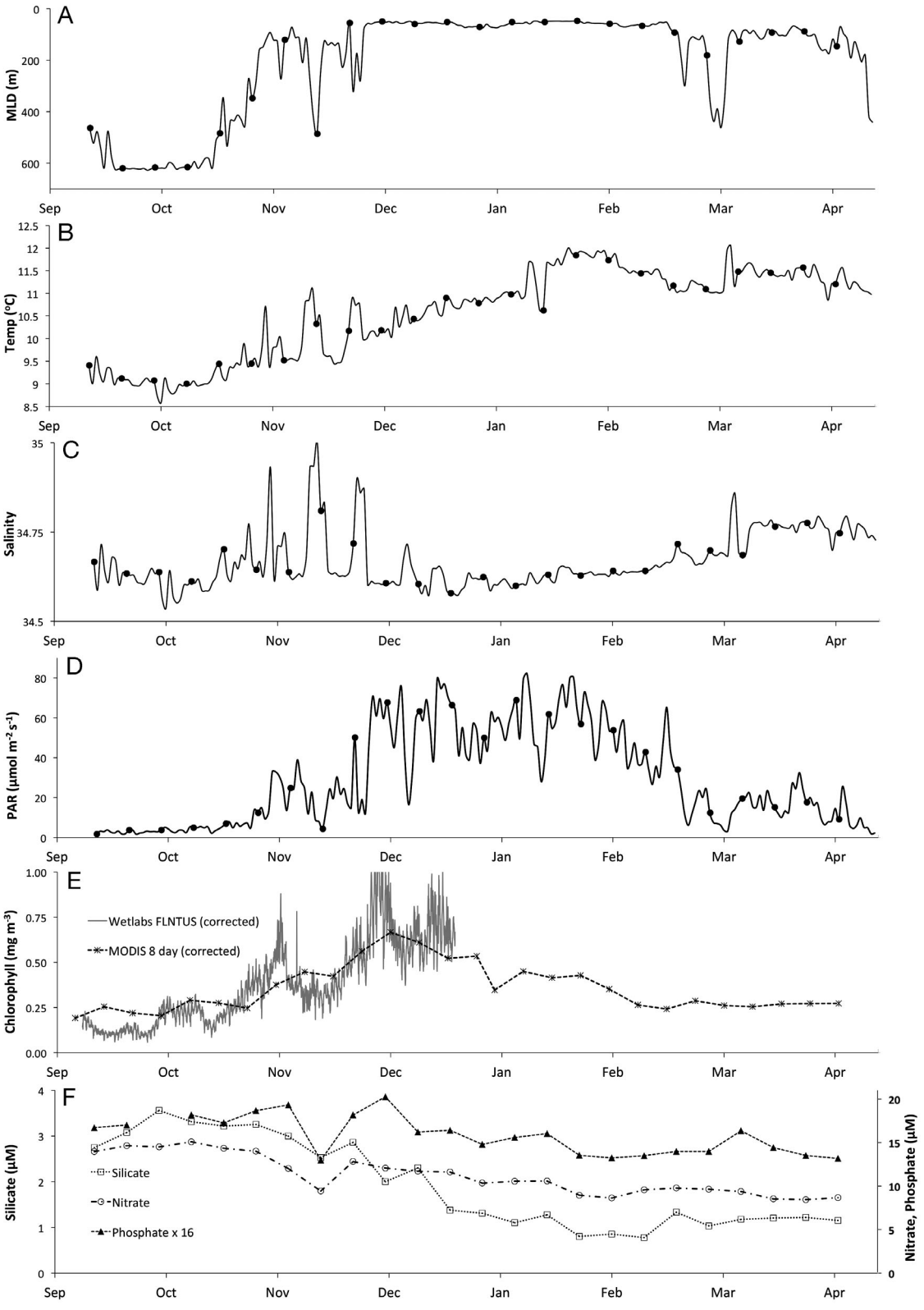

Fig. 3. Pulse 7 time-series of (A) mixed-layer depth (MLD), (B) temperature, (C) salinity, (D) photosynthetically active radiation (PAR; averaged over the MLD) (E) chlorophyll (Wetlabs FLNTUS and MODIS) and (F) nutrients. Note that phosphate data are multiplied by the Redfield ratio to more clearly show the seasonal change. (A–D) Individual sample dates are shown as filled circles superimposed on the sensor data. Data for B–F were collected at 32 m depth

renewal of surface ocean nutrients through winter until stratification recommences in early spring (Shadwick et al. 2015). Depletions of all 3 nutrients were substantial over the season, and similar to previous estimates based on a seasonal cycle assembled from data across multiple years (Lourey & Trull 2001). Nitrate decreased from approximately 15 to 9 µM. Based on the observed salinity increase over this period, approximately 20% of this decrease is likely to have been derived from increasing summer supply of oligotrophic subtropical waters (Lourey & Trull 2001). Phosphate depletion was linearly correlated with the nitrate depletion with a ratio of 12.9 ± 2.3 (R^2 = 0.602), i.e. somewhat lower than the global average Redfield ratio of 16, but similar to previous observations in the Subantarctic and Polar Frontal Zone south of Australia (Lourey & Trull 2001). The end of summer nitrate and phosphate levels remained well above limiting concentrations for phytoplankton growth (Bowie et al. 2011). In contrast, silicate depletion did reach limiting levels, decreasing from 3.6 µM in early spring to 0.8 µM in mid-summer, i.e. very close to the level of 0.7 µM below which it appears that diatoms cannot further decrease silicate (Paasche 1973). The nitrate/silicate depletion ratio over the deployment was 2.1 ± 0.23 (R^2 = 0.795) and thus well above values of 0.25–0.5 expected for a diatom-dominated community (Takeda 1998, Ragueneau et al. 2006), indicating the importance of other organisms in the seasonal uptake and export of nutrients. The depletion of nutrients was most rapid from early November through mid-December (Fig. 3F), consistent with surface-layer-oxygen-budget based estimates of net community production (NCP), which indicated production increased before and during spring stratification followed by summer-time cessation of NCP (Weeding & Trull 2014). The role of resupply of nutrients by mixing across the base of the mixed layer is most important in this spring period; sufficient that the actual biological drawdown of nitrate and phosphate may be ~50% higher than the water column depletion, with this effect decreasing to ~10% in summer (Wang et al. 2001).

Phytoplankton community structure

Data are presented as both abundance (cells l^{-1}; Fig. 4A,B) and biovolume (µm^3 l^{-1}; Fig. 4C,D) because these metrics have differing implications for conceptual models of trophodynamics and carbon export from surface waters. The relative sizes and estimated biovolumes of the major groups highlights variations in cell size from 3 to 200 µm, and an associated 4–5 orders of magnitude variation in biovolume (Fig. S2 in the Supplement). Small cells at the limit of reasonable discrimination by light microscopy (2–5 µm) may include a wide variety of species, including parmales, diatoms, coccolithophores, flagellates, chlorophytes, cyanobacteria, and choanoflagellates.

Taxa abundances

Total phytoplankton abundance (cells l^{-1}) for the main groups (diatoms, dinoflagellates, silicoflagellates, flagellates, loricate [tintinnid] and naked ciliates, and unidentified 'other' group) for the 24 samples in the time series show that with the exception of tintinnids and silicoflagellates, all major groups were present in each sample (Fig. 4A). Total phytoplankton abundance was lowest at the start of the deployment (early spring), and increased by ~2 orders of magnitude over the entire sampling period, concomitant with the smaller increase (~5-fold) in chlorophyll observed in both satellite and sensor data (Fig. 3E). All samples were dominated by flagellates, primarily the motile form of the autotrophic haptophyte *Phaeocystis antarctica*, with a minor contribution of *Phaeocystis scrobiculata*, and unidentified nanoflagellates. The percentage of *P. antarctica* was initially low (average 22%) in September 2010, but was more typically 50–75% of the total cell count for the majority of the deployment period. Overall, the community abundance was dominated by autotrophs, with a small (2-fold) increase in species richness (*S*) over the period of the deployment (Fig. 4A).

Diatoms and dinoflagellates followed similar patterns of abundance, with low initial concentrations, increasing in abundance with increasing water temperature, shoaling MLD, and the drawdown of nutrients throughout spring and summer. The highest abundances of both diatoms and dinoflagellates were observed in late summer; however, the proportion of these groups together rarely exceeded 25% of the total abundance. Variations in the diatom:dinoflagellate ratio were generally small (Fig. 4E), with the greatest variation arising during the period of MLD instability in September 2010. The maximum ratio of diatoms to dinoflagellates (5:1) occurred when silicate concentration (3.6 µM) peaked in the sample collected on 30 September 2010.

Ciliates rarely contributed more than 10% to total abundance (Fig. 4B), except in the first samples collected in early spring. By early December, ciliates

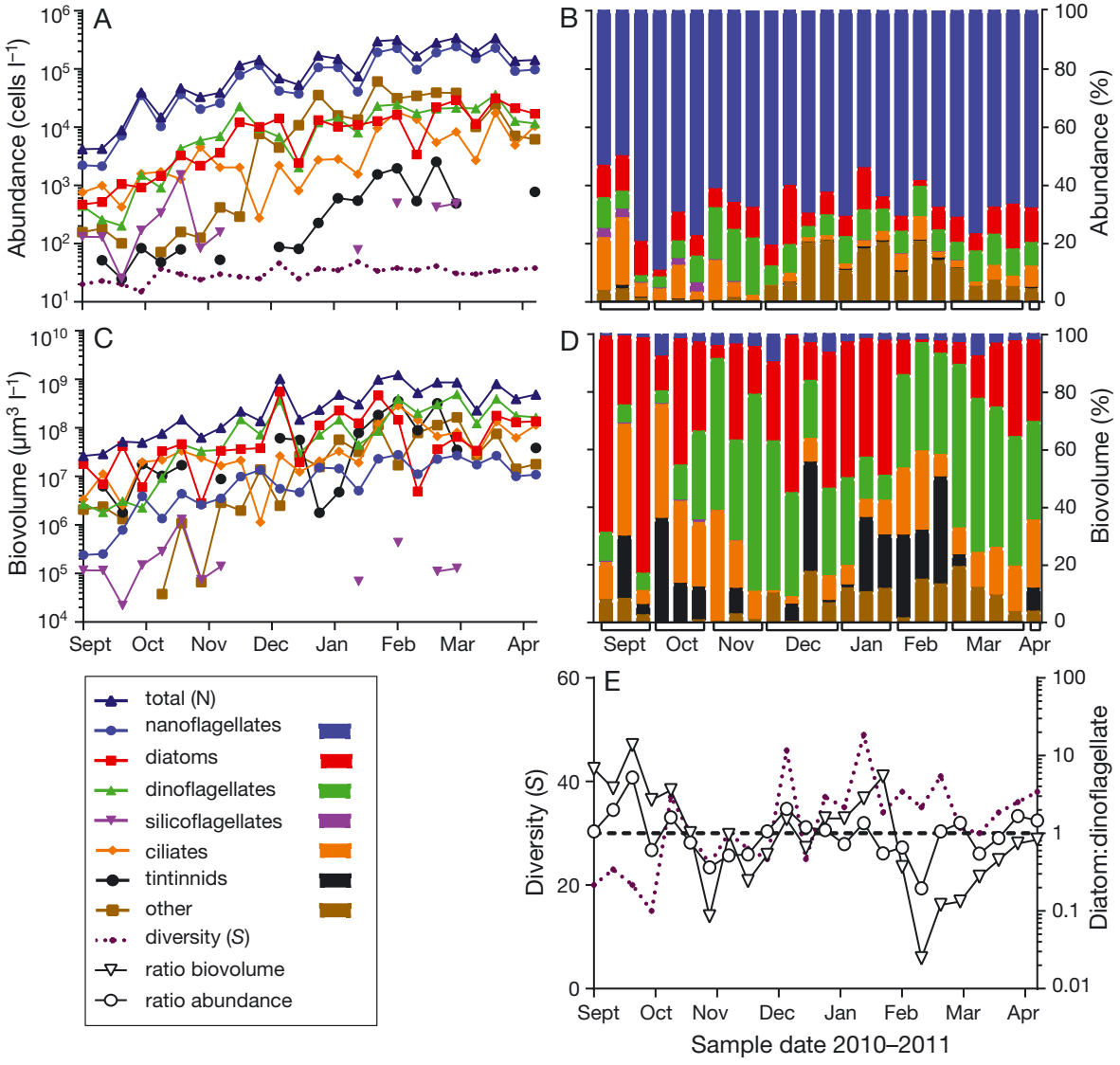

Fig. 4. Pulse-7 phytoplankton samples collected at 9-d intervals from September 2010 to April 2011 showing major group (A) abundance (cells l^{-1}), (B) % abundance, (C) biovolume (µm^3 l^{-1}), (D) % biovolume and (E) ratio of diatoms:dinoflagellates (biovolume and abundance) and number of species (diversity, *S*). Note the log scale for A, C and E (diatom:dinoflagellate ratio)

were absent, and typically contributed less than 5% of the total abundance for the remainder of the deployment, coincident with increases in the 'other' category. Large loricate ciliates (tintinnids) were rarer still and completely absent from the samples for periods in November, December and March. Tintinnid genera present included *Ascambeliella*, *Dictyocysta*, *Epiplocylis*, *Eutintinnus*, *Parundella*, *Rhabdonella*, *Salpingella* and *Steenstrupiella*. Silicoflagellates (in the skeleton-bearing state) were the rarest category of microplankton, with *Stephanocha speculum* and *Dictyocha stapedia* present in early samples, but only sporadically observed once silicate concentrations dropped below ~2 µM in summer.

Taxa biovolumes

Total biovolume (µm^3 l^{-1}) increased steadily throughout spring, reaching a 'peak' in early December (Fig. 4C) with contributions from large diatom species (*Corethron*, *Coscinodiscus*), gymnodinioids, and armoured dinoflagellates (*Oxytoxum*, *Protoperidinium*, *Prorocentrum*). The highest diatom biovolume occurred in late September, with 75% of the total biovolume attributed to the large centric species *Proboscia alata*, *Corethron pennatum*, and *Thalassiosira* spp. A similar level of total biomass was achieved in late January/early February; however, the contribution of diatoms to total biovolume was highly

variable, as the proportion of tintinnids and aloricate ciliates increased. The maximum diatom:dinoflagellate biovolume ratio (14:1) occurred at the same time as the corresponding maximum abundance ratio (Fig. 4E).

The community at the end of summer was dominated by diatoms (*Leptocylindrus mediterraneus*, *Proboscia alata*) that appeared more weakly silicified than in earlier samples, dinoflagellates (*Tripos pentagonus/lineatus* complex, *Oxytoxum, Protoperidinium*), and *Strombidium*-like ciliates. Nanoflagellates were the most abundant group; however, *Phaeocystis* and other nanoflagellates contributed less than 3% to the total biovolume (Fig. 4D). Silicoflagellates in the skeleton-bearing stage were also a very minor contributor to total biovolume, owing to both their low concentrations and relatively small biovolume (Fig. S2 in the Supplement). At the conclusion of the deployment (April 2011), total biovolume declined as MLD began to destabilize, accompanied by slight decreases in water temperature and salinity (Fig. 3). Neither abundance nor biovolume data showed a clear response to the transient passage of warm, salty, low-nutrient water parcels identified in Fig. 3.

Seasonal groupings

Cluster analysis of community abundance data (Fig. 5A) displays the overall similarity between pairs of samples over the deployment. The dendrogram is arbitrarily rotated to display a largely chronological order for ease of comparison with the time-series plots, but the critical feature is the groupings of samples, and the similarity level at which each group is formed. Three main groups were delineated at 47% similarity: early and late spring groups and a combined summer/autumn group (stress = 0.12). Cluster analysis of biovolume data (not shown) showed 3 very similar seasonal groupings (2 spring groups, and autumn tightly clustered within a broader summer group), although the delineation was at 41% similarity. The nMDS based on abundance was mutually consistent with the cluster analysis and confirmed the representation of seasonal groupings (Fig. 5B). The time trajectory shown on the nMDS for abundance data shows the seasonal groups coincided with a shift from deep MLD to a stable MLD. The global R-value for the ANOSIM routine was 0.952, rejecting the null hypothesis that there was no difference in assemblages in abundance groups based on MLD (deep, stratifying, stable/shallow) at the significance level of $p < 0.01$.

Although the physical and chemical variables measured clearly captured the temporary presence

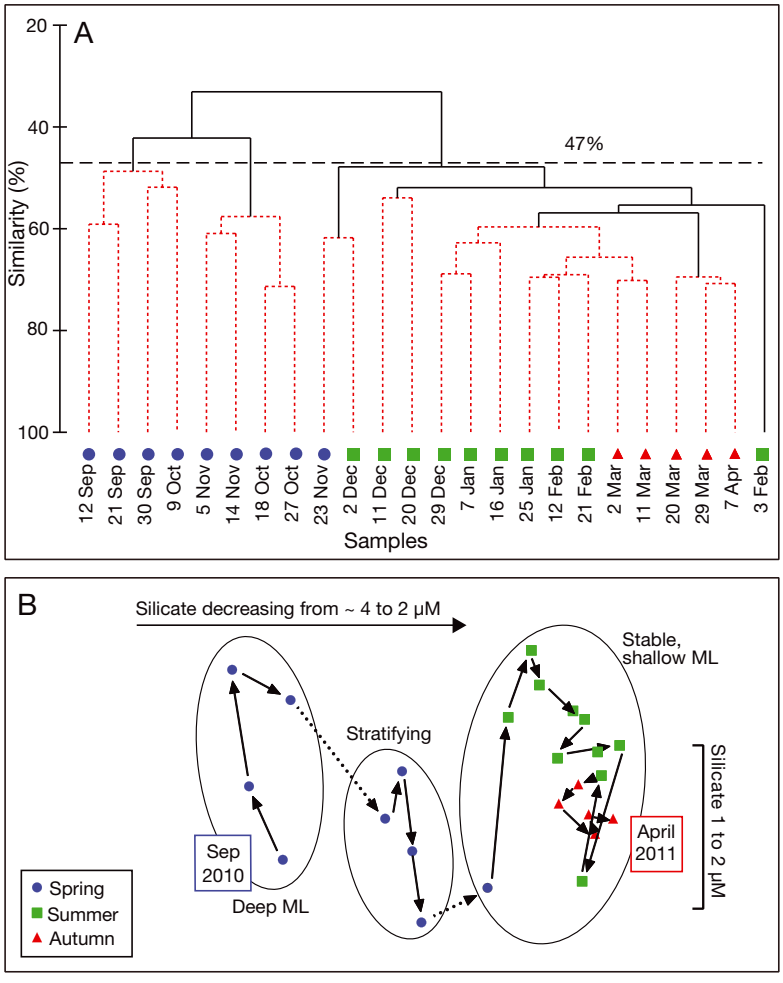

Fig. 5. (A) Group-averaged hierarchical cluster of phytoplankton species (abundance, cells l^{-1}), using the Bray-Curtis similarity index (cluster delineation at 47%, stress = 0.12). Red lines indicate samples within that structure cannot be significantly differentiated, based on SIMPROF analysis. Biovolume data showed similar grouping of samples, with spring split into 2 groups and a combined summer/autumn group. (B) Non-metric multidimensional scaling (nMDS) ordination of phytoplankton community data (abundances). Data were 4th root transformed, using the Bray-Curtis similarity index (stress = 0.12). Dotted lines and arrows indicate the trajectory of the time series starting September 2010 and ending April 2011; ellipses indicate groupings from the cluster analysis

of warmer, saltier, low-nutrient water in late spring, the phytoplankton community composition did not shift in any demonstrable way, suggesting that small variations in warming were not a dominant control on community structure.

Species contributing to seasonal groupings

Species contributions to the 3 groups (early spring, late spring, summer/autumn) calculated by SIMPER analysis identified *Phaeocystis antarctica* as the species with the largest contribution to the average similarity within each group (Table 1), reflecting its abundance in all samples. A small increase in diversity in the groups is reflected by an increase in the number of discriminating species contributing to the cumulative similarity (cut-off at 50%), with a corresponding decrease in the contribution of *P. antarctica* to the overall similarity within each group. The early spring cluster was characterized by *Phaeocystis*, fusiform flagellates and *Thalassiosira* (20–30 µm), and the occurrence of the silicoflagellate *S. speculum*, which cumulatively accounted for 50% of the overall similarity of these samples. Interestingly, pollen (*Pinus* spp.) was also a contributor, albeit minor, suggesting a potential influence from seasonal wind patterns. Few diatom taxa were present in the SIMPER groups, other than small *Thalassiosira* (20–30 µm) in early spring, and the smaller size class URGO category (<5 µm) in summer/autumn, which contained many very small diatoms such as *Minidiscus* and smaller *Fragilariopsis* species, resolved only with SEM and the subject of more discrimination in later deployments. Late spring was characterized by a slightly more diverse community with more dinoflagellate species (*Prorocentrum*, *Scripsiella*, *Oxytoxum*, *Protoperidinium*) contributing to the group similarity, in addition to a smaller size class of *Thalassiosira* and fewer silicoflagellates. The summer/autumn cluster included contributions from a greater number of heterotrophic and mixotrophic taxa (including unidentified heterotrophs of 10–20 µm and 20–30 µm size, and *Strombidium*), as well as *Mesodinium* and the URGO class containing small diatoms.

Diatom species community composition

Although diatoms were a numerically minor contributor to total abundance, their total biovolume was large, typically 20–50% of the total and occasionally

Table 1. Contributions to average group similarity, expressed as average abundance per group, average contribution to group similarity (highest to lowest), ratio of contribution to standard deviation (SD), individual % contribution to the group similarity and cumulative % similarity (cut-off 50%), according to SIMPER analysis. ML: mixed layer; URGO: unidentified round green object

Contribution	Average abundance	Contribution to group similarity	Similarity/SD	% Contribution	Cumulative %
Early spring (deep ML) average similarity 50.97					
Phaeocystis antarctica	8.13	8.71	5.14	17.09	17.09
Fusiform flagellate 5–10 µm	6.86	8.64	19.94	16.95	34.03
Thalassiosira small (20–30 µm)	3.16	4.24	16.45	8.33	42.36
Stephanocha speculum	3.15	4.07	4.43	7.99	50.35
Late spring (stratifying ML) average similarity 56.89					
Phaeocystis antarctica	12.34	8.14	8.53	14.30	14.30
Round flagellate 5–10 µm	7.47	5.00	11.87	8.79	23.10
Fusiform flagellate 5–10 µm	6.72	4.23	11.35	7.43	30.53
Strombidium spp.	4.73	3.04	5.28	5.34	35.87
Prorocentrum spp.	4.58	2.87	6.03	5.05	40.92
Scrippsiella trochoidea	4.26	2.85	8.91	5.02	45.94
Oxytoxum spp.	4.40	2.56	3.33	4.49	50.43
Summer/autumn (stable ML) average similarity 56.60					
Phaeocystis antarctica	17.59	7.19	6.75	12.70	12.70
Round flagellate 5–10 µm	9.45	3.80	8.17	6.72	19.42
Unidentified heterotrophs 10–20 µm	9.12	3.52	5.62	6.22	25.64
Fusiform flagellate 5–10 µm	8.42	3.31	6.98	5.85	31.49
URGO <5 µm	7.59	2.97	9.16	5.24	36.73
Oxytoxum spp.	7.25	2.91	6.73	5.14	41.86
Gymnodinioid 10–15 µm	7.05	2.79	4.37	4.93	46.79
Mesodinium rubrum	6.38	2.42	5.76	4.28	51.07

exceeding 75% (Fig. 4C,D). Species composition in the early spring included small *Thalassiosira* (<30 µm diameter), *Leptocylindrus mediterraneus* (almost always colonised by the epiphytic stramenopile *Solenicola setigera*), and minor contributions to total abundance from pennate genera such as *Ceratoneis*, *Fragilariopsis*, *Navicula*, *Nitzschia*, and *Thalassiothrix*. Rarer taxa such as *Planktoniella sol*, *Asteromphalus parvulus*, and *Proboscia alata* appeared sporadically, generally later in the time series. *Fragilariopsis kerguelensis*, a commonly observed SO phytoplankton (Cortese & Gersonde 2007) was present only as fragments or associated with faecal pellets, possibly indicating the limits of its temperature niche, or preferential grazing by zooplankton resulting in very low standing stocks (Rigual-Hernandez et al. 2015).

Throughout summer, small centric diatoms were an important contributor to total diatom abundance, with a decrease in the size class observed in November–December (<10 µm diameter) to <5 µm diameter in December–February. Greater resolution of these smaller size classes using SEM analysis will be pursued in subsequent deployments.

Influence of environmental variables

We explored possible relationships between biotic and abiotic data, to assess how community patterns are aligned with expectations about the major drivers of phytoplankton community composition (turbulence, nutrients). Comparison of the species similarity matrices (using all 108 taxa) with the environmental variable matrices (Table 2) shows that for single variables, silicate, MLD, temperature, and nitrate provided the highest rank correlations. Considering pairs of variables improved the correlations by more than 10%, with similar correlation strengths for silicate, temperature, and nitrate, all paired with MLD. Adding a third variable produced only very small correlation increases. Average mixed-layer PAR, chlorophyll concentrations, and salinity showed the poorest correlations.

DISCUSSION

We compare our results to previous observations in the SAZ, at the levels of major groups and then the siliceous species. We then consider the high temporal resolution seasonal cycle provided by the autonomous sampler, and its relationships to environmental conditions, trophodynamics, and the potential implications for carbon export and cycling of nutrients in the SAZ. In seeking to answer the questions we posed in the 'Introduction', we note that resolution of the complete protist community is made difficult by the wide range of cells sizes present (picoplankton 0.2–2 µm; nanoplankton 2–20 µm; microplankton 20–200 µm; and mesoplankton 200–2000 µm), and the limitations of our sampling, preservation, and light microscopy techniques.

What is the composition of the phytoplankton community in the SAZ?

The subdued seasonality exhibited in the phytoplankton community at the SOTS observatory is most evident in the absence of a classical spring bloom. The general community structure we observed is consistent with other temporally limited, but broader spatial surveys of the region, with some differences.

Table 2. Results of BEST analysis for single, double and triple subsets of environmental variables measured at the Southern Ocean Time Series deployment, 2010–2011. The Spearman rank correlation for the variable(s) yielding the best matches between the community and environmental similarity matrices is shown. MLD: mixed-layer depth; PAR: photosynthetically active radiation

Run	One variable	Corr	Two variables	Corr	Three variables	Corr
1	Silicate	0.769	Silicate + MLD	0.869	Silicate + Nitrate + MLD	0.880
2	MLD	0.730	Temperature + MLD	0.860	Silicate + Temperature + MLD	0.872
3	Temperature	0.717	Nitrate + MLD	0.850	Temperature + Nitrate + MLD	0.850
4	Nitrate	0.699	Silicate + Nitrate	0.804	Phosphate + Silicate + MLD	0.802
5	Phosphate	0.343	Silicate + Temp	0.786	Silicate + Chlorophyll + MLD	0.797
6	PAR_{MLD}	0.254	Phosphate + MLD	0.749	Silicate + Nitrate + PAR_{MLD}	0.792
7	Chlorophyll	0.062	Nitrate + Temp	0.721	Silicate + Nitrate + Temp	0.791
8	Salinity	0.042	Nitrate +PAR_{MLD}	0.695	Phosphate + Temperature + MLD	0.789

The autotrophic haptophyte *Phaeocystis antarctica* dominated sample abundances throughout the deployment, although we only observed the solitary motile phase, not the colonial form. Studies in the SAZ by Kopczynska et al. (2007) and de Salas et al. (2011) recorded mixed phytoplankton communities with abundances dominated by prymensiophyte nanoflagellates, while Iida & Odate (2014) used pigment analyses to show that *P. antarctica* represented between 30 and 75% of total chlorophyll biomass in the summer. Recent re-analysis of the SAZ-SENSE data including CHEMTAX analysis of phytoplankton pigments by Cassar et al. (2015) and re-examination of microscopy samples (R. Eriksen unpubl. data) also support a large standing stock of *Phaeocystis* in the SAZ. *Phaeocystis* is observed to recurrently bloom in the polar SO (DiTullio et al. 2000), and may occur as different morphologies — solitary forms or colonies. The solitary form is more common under conditions of iron limitation (Schoemann et al. 2005), although this may also reflect grazing pressure (Tang 2003). There are potential implications for carbon removal mechanisms associated with the dominant morphology, as up to 50% of the carbon mass of *P. antarctica* is allocated to the extracellular mucus of the colonial matrix (DiTullio et al. 2000). Notably, we observed no colonial forms, consistent with low iron availability.

Flow cytometry data (Cassar et al. 2015) showed that small cyanobacteria contributed up to 20% of identified biomass across the SAZ. This size class (<2 µm diameter) is beyond the practical resolution of light microscopy and thus not quantified here, but reinforces the importance of assessing the picoplankton in understanding community composition in the SAZ. Other species beyond the practical resolution of light microscopy include the coccolithophores. Although recognized as an important indicator of ocean acidification impacts (Deppeler & Davidson 2017), their overall contribution to total abundance in the SAZ has been shown to be small (Iida & Odate 2014, Trull et al. 2018) and variable (Cubillos et al. 2007, Kopczynska et al. 2007; S. Wright, Australian Antarctic Division, unpublished pigment data).

Primary production in the SO is widely reported to be dominated by diatoms, but this is probably most true of polar waters, and less so of Subantarctic waters. We observed diatoms to be a relatively small component of the total community abundance, coexisting with other groups. This is consistent with previous work south of Australia (Kopczynska et al. (2007), where *Pseudo-nitzschia*, *Nitzschia*, *Rhizosolenia*, and *Fragilariopsis* were observed to occur in low numbers; however, in contrast, we did not observe any diatom resting stages in our samples. Formation of resting stages in diatoms have been linked to both iron and nitrate depletion (typically following a spring bloom), and can significantly alter the density and sinking rate of cells and export of carbon through development of heavily silicified spore frustules (Sugie & Kuma 2008).

How does this community vary seasonally?

From an abundance perspective, the succession of major groups over the deployment was subdued. With the exception of the silicoflagellates, which were present in late winter and early spring, and sporadic records of tintinnids, all groups were represented in all samples. At the species level, there were subtle changes in the composition of the major clusters identified, and these could be tied to 3 distinct stages in the development of the mixed layer: early spring (deep mixed layer), late spring (stratifying mixed layer), and a longer period of stable mixed layer in summer/autumn. Species richness increased modestly, and the contribution of *P. antarctica* to group similarity decreased throughout the deployment, while the number of other taxa contributing to the similarity within groups increased.

Conversion to biovolume offers us a different perspective on the successional changes in the community. Diatoms and dinoflagellates combined to typically represent between 40 and 90% of the total biovolume, with ciliates (loricate and aloricate) the other major contributor. Diatoms have been described as ubiquitous generalists (r strategists), while dinoflagellates are more responsive to niche changes (K strategists), and with the exception of silicate, these 2 phytoplankton groups are reported to have basically comparable nutrient requirements, with the potential to substitute for each other in biogeochemical cycles (Klais et al. 2011). The ratio of diatom to dinoflagellate biovolumes in early spring favoured the diatoms, and decreased rapidly during stratification, before stabilizing near 1 in early summer and then decreasing further towards the end of the record. Under conditions of the stable mixed layer over summer, dinoflagellates contributed proportionally more to total biovolume than diatoms. This seasonal sequence of succession from diatoms towards dinoflagellates is a core aspect of the phenology developed by Margalef (1978), based on resource limitation in summer, which dinoflagellates overcome via their motility. However, in the very deep SAZ mixed layers, with the presence of abundant phosphate and

Table 3. Correlation coefficients (Pearson's r) between environmental variables recorded at the Southern Ocean Time Series site during the Pulse 7 deployment ($^{*}p < 0.05$, $^{**}p < 0.01$). MLD: mixed-layer depth; PAR_{MLD}: photosynthetically active radiation averaged over the MLD

	Phosphate	Silicate	Nitrate	MLD	Temperature	Salinity
Silicate	0.703**					
Nitrate	0.776**	0.892**				
MLD	0.232	0.772**	0.714**			
Temperature	−0.740**	−0.953**	−0.914**	−0.778**		
Salinity	−0.461*	−0.073	−0.404	0.079	0.236	
PAR_{MLD}	0.051	−0.495*	−0.305	−0.764**	0.440*	−0.540**

nitrate, this is not an obvious explanation. Instead, the sequence may reflect the depletion of silica and its limitation of diatom abundance and size. This view is consistent with the lack of any strong seasonality in the numerical abundance of dinoflagellates relative to diatoms. Dinoflagellates are often observed to inhibit cell division during turbulent events, dividing rapidly during periods of calm after a high level of turbulence (Thomas et al. 1995). A small injection of silicate in late autumn saw an increased contribution from diatoms to biovolume, although the ratio continued to favour the dinoflagellates.

How are the seasonal taxonomic variations influenced by environmental conditions?

Our analysis identified significant correlations between seasonal community composition variations and environmental variabilities, in particular, silicate and MLD, but also temperature and nitrate. Because all these variables are also correlated with each other (Table 3), owing to the dominance of the seasonal cycle in their signals, evaluation of their relative potential importance to community composition benefits from consideration of possible mechanisms of control and associated amplitudes. Before addressing this, we note that salinity did not present as an important correlate with community composition, and thus inputs of subtropical water do not appear to have had a significant influence (a point that also emerged from the lack of community composition changes in November, when parcels of high-salinity water passed the site).

Nitrate concentration remained non-limiting throughout the deployment, and thus it seems unlikely that this was a direct influence. It is possible that nitrate (and phosphate) depletion might serve as a proxy for iron depletion, which is known to reach limiting levels at this site by mid-summer (Bowie et al. 2009, Lannuzel et al. 2011) and quite possibly much sooner in the season (Sedwick et al. 2008). The observed magnitude of nitrate depletion was sufficient to indicate complete iron depletion by mid-summer (0.2 nM Fe consumption after 3 µM nitrate consumption), based on a moderate Fe/N depletion ratio (10 µmol Fe/mole C at Redfield C/N; de Baar et al. 1995, Maldonado et al. 2001).

The maximum temperature range observed (3.5°C) at the SOTS site was likely too small to be a significant influence compared to the boundaries of the temperature niche widths of phytoplankton taxa in temperate parts of the SO (Norberg 2004, Boyd et al. 2013, Thomas et al. 2016). Thus, as with nitrate, the correlation of community diversity with temperature may reflect other seasonal controls, and a direct influence is unlikely. The amount of PAR available to the phytoplankton community was controlled by MLD, as described above, and the variations were substantial, from growth-limiting levels in winter to moderate levels in summer. This might be expected to be a key mechanism by which MLD affects community composition, but the average PAR in the MLD was not identified by the BEST analysis as an important variable. This could reflect similar light requirements across the taxa, or of course other impacts on their accumulation, for example, the influence of MLD on removal by grazing (which we cannot evaluate from our observations).

Silicate emerged as having a very strong influence on community structure. As noted in the 'Results' section, this is consistent with drawdown to below 1 µM, considered to be limiting to diatoms. Silicate levels were also linked to the presence of silicoflagellates, which were observed mainly in late winter and early spring, when silicate levels were at their highest. Changes in diatom size and silicification were observed later in the year, with the appearance of smaller, more weakly silicified centric diatoms in summer. Silicate drawdown, in contrast to nitrate limitation, has previously been shown to lead to more lightly silicified cells (Davis & Hildebrand 2010, de Salas et al. 2011, Fripiat 2011), and to have a profound effect on growth rates and both abundance and species composition (Leblanc & Hutchins 2005). Rapid recycling of silicate would also be necessary to sustain siliceous species in any numbers under conditions of limited supply (Queguiner 2001). Takeda

(1998) observed changes in diatom cells under iron limitation, tending towards smaller cell volumes with higher silica contents per cell. Thus, changes to diatom silicification may occur as a direct result of silica availability, and/or via the influence of iron depletion.

No significant correlation of community structure with total chlorophyll biomass was observed, presumably as a result of the small seasonal improvement in growth conditions, which failed to produce a strong spring bloom, and which led to only moderate biomass increase. These 'bottom-up' controls on community composition phenology may of course be modified by 'top-down' selective feeding (Mariani et al. 2013), an issue for which we do not have data to address and, accordingly, must remain unresolved.

How might the community structure influence the biological carbon pump?

We observed a high nitrate/silicate drawdown ratio, well above that expected for dominance of export by diatoms on their own. This means that the nanoplankton-dominated communities in the SAZ are capable of making significant contributions to carbon export, even under conditions of limited iron availability. This has been emphasized recently in this region, based on net community production results and their comparison to pigment compositions in late summer (Cassar et al. 2015), and was previously inferred from global median levels of organic carbon export to deep sediment traps unaccompanied by biogenic silica (Trull et al. 2001a). As we have now shown, this export observed by others using traps (Trull et al. 2001a, Ebersbach et al. 2011), net community production methods (Weeding & Trull 2014, Cassar et al. 2015), and pCO_2 observations (Shadwick et al. 2015) occurs despite the lack of a strong spring bloom, emphasizing that decoupling of production and grazing is not always required to achieve significant biological carbon sequestration.

CONCLUSIONS

Our study in the surface waters of the SAZ captured community composition over a spring–summer–autumn cycle, and showed that the phytoplankton community abundance at the SOTS site was dominated throughout the deployment by the autotrophic haptophyte *P. antarctica*, primarily in the solitary flagellate form. Diatoms were a small component numerically, but were important from a biovolume perspective, with changes in the size and degree of silicification as silica in the water column was depleted. Other siliceous algae such as silicoflagellates in the skeleton-bearing stage also responded to silica drawdown.

Although there were no dramatic shifts in community composition over the period of the deployment, the phytoplankton community structure was linked to the depth of the mixed layer, with samples clustering as spring assemblages (MLD > 500 m), or summer/autumn assemblages (MLD < 50 m). The sensor array picked up passage of several distinct water parcels in spring, but these short-term events were not reflected by changes in the phytoplankton community composition. The overall subdued seasonality is interesting given the observed seasonal depletion of dissolved silica and, presumably, dissolved iron based on previous work (Sedwick et al. 2008, Bowie et al. 2011). It suggests that efficient recycling of these elements may be a key moderator of changes in seasonal community composition. Coupling of this time series with later deployments at the SOTS site will shed further light on the representativeness of our results, and further improve our understanding of the controls on phytoplankton abundance, diversity, and controls on succession.

Acknowledgements. The Southern Ocean Time Series Observatory is a facility of the Australian Integrated Marine Observing System (www.imos.org.au), and receives additional logistical and financial support from the Antarctic Climate & Ecosystems Cooperative Research Centre, CSIRO Oceans and Atmosphere, Bureau of Meteorology, Australian Marine National Facility, and Australian Antarctic Division (AAD) (AAS Awards 1156, 2256 and 4352 to T. Trull). Participation of the ACE CRC is supported by the Australian Commonwealth Collaborative Research Centres Program. We thank our ACE CRC and CSIRO mooring specialists and the captains and crews of the RV 'Southern Surveyor' and RV 'Aurora Australis' for their efforts during mooring deployment and recovery voyages. Dr Christina Schallenberg (ACE CRC) provided expertise on the adjustment factors for satellite and *in situ* chlorophyll data. We are grateful to Fiona Scott and Imojen Pearce (AAD) for feedback on identification of Southern Ocean protists, Simon Wright (AAD) for access to L'Astrolabe coccolithophore data, Kerrie Swadling (Institute for Marine and Antarctic Studies) for suggestions on multivariate analysis, Leanne Armand and Andrés Rigual-Hernández (Macquarie University) for many discussions on the SOTS diatom community, Abe Passmore (CSIRO) for mapping the frontal positions, and Val Latham (CSIRO) for nutrient analysis. The manuscript was strengthened considerably by comments from Dr Kristen Karsh, Professor Phil Boyd (both University of Tasmania) and 4 anonymous reviewers.

LITERATURE CITED

Arrigo KR, Robinson DH, Worthen DL, Dunbar RB, DiTullio GR, VanWoert M, Lizotte MP (1999) Phytoplankton community structure and the drawdown of nutrients and CO_2 in the Southern Ocean. Science 283:365–367

Assmy P, Smetacek V, Montresor M, Klaas C and others (2013) Thick-shelled, grazer-protected diatoms decouple ocean carbon and silicon cycles in the iron-limited Antarctic Circumpolar Current. Proc Natl Acad Sci USA 110: 20633–20638

Banse K (1996) Low seasonality of low concentrations of surface chlorophyll in the Subantarctic water ring: underwater irradiance, iron or grazing? Prog Oceanogr 37: 241–291

Behrenfeld MJ (2014) Climate-mediated dance of the plankton. Nat Clim Chang 4:880–887

Bender M, Tilbrook B, Cassar N, Jonsson B, Poisson A, Trull TW (2016) Ocean productivity south of Australia during spring and summer. Deep-Sea Res I 112:68–78

Blain S, Queguiner B, Armand L, Belviso S and others (2007) Effect of natural iron fertilization on carbon sequestration in the Southern Ocean. Nature 446:1070–1074

Bowie AR, Lannuzel D, Remenyi TA, Wagener T and others (2009) Biogeochemical iron budgets of the Southern Ocean south of Australia: decoupling of iron and nutrient cycles in the subantarctic zone by the summertime supply. Global Biogeochem Cycles 23:GB4034

Bowie AR, Brian Griffiths F, Dehairs F, Trull TW (2011) Oceanography of the Subantarctic and Polar Frontal Zones south of Australia during summer: setting for the SAZ-Sense study. Deep-Sea Res II 58:2059–2070

Boyd PW, Doney SC (2002) Modelling regional responses by marine pelagic ecosystems to global climate change. Geophys Res Lett 29:53-1–53-4

Boyd PW, Doney SC (2003) The impact of climate change and feedback processes on the ocean carbon cycle. In: Fasham MJR (ed) Ocean biogeochemistry — the role of the ocean carbon cycle in global change. Springer-Verlag, Berlin, p 157–193

Boyd PW, Doney SC, Strzepek R, Dusenberry J, Lindsay K, Fung I (2008) Climate-mediated changes to mixed-layer properties in the Southern Ocean: assessing the phytoplankton response. Biogeosciences 5:847–864

Boyd PW, Rynearson TA, Armstrong EA, Fu F and others (2013) Marine phytoplankton temperature versus growth responses from polar to tropical waters — outcome of a scientific community-wide study. PLOS ONE 8:e63091

Cassar N, Wright SW, Westwood KJ, De Salas M and others (2015) The relation of mixed-layer net community production to phytoplankton community composition in the Southern Ocean. Global Biogeochem Cycles 29:446–462

Clarke KR (1993) Non-parametric multivariate analyses of changes in community structure. Aust J Ecol 18:117–143

Clarke KR, Ainsworth M (1993) A method of linking multivariate community structure to environmental variables. Mar Ecol Prog Ser 92:205–219

Clarke KR, Gorley RN (2006) PRIMER v6: User Manual/Tutorial. PRIMER-E, Plymouth

Cornet-Barthaux V, Armand L, Quéguiner B (2007) Biovolume and biomass estimates of key diatoms in the Southern Ocean. Aquat Microb Ecol 48:295–308

Cortese G, Gersonde R (2007) Morphometric variability in the diatom *Fragilariopsis kerguelensis*: implications for Southern Ocean paleoceanography. Earth Planet Sci Lett 257:526–544

Cubillos JC, Wright SW, Nash G, de Salas MF, Griffiths B, Tilbrook B, Poisson A, Hallegraeff GM (2007) Calcification morphotypes of the coccolithophorid *Emiliania huxleyi* in the Southern Ocean: changes in 2001 to 2006 compared to historical data. Mar Ecol Prog Ser 348:47–54

Davies CH, Coughlan A, Hallegraeff G, Ajani P and others (2016) A database of marine phytoplankton abundance, biomass and species composition in Australian waters. Sci Data 3:160043

Davis AK, Hildebrand M (2010) Molecular processes of biosilicification in diatoms. Biomineralization. John Wiley & Sons

de Baar HJW, de Jong JTM, Bakker DCE, Loscher BM, Veth C, Bathmann U, Smetacek V (1995) Importance of iron for phytoplankton blooms and carbon dioxide drawdown in the Southern Ocean. Nature 373:412–415

de Salas MF, Eriksen R, Davidson AT, Wright SW (2011) Protistan communities in the Australian sector of the Sub-Antarctic Zone during SAZ-Sense. Deep-Sea Res II 58:2135–2149

Deppeler S, Davidson A (2017) Southern Ocean phytoplankton in a changing climate. Front Mar Sci 4:1–28

DiTullio GR, Grebmeier JM, Arrigo KR, Lizotte MP and others (2000) Rapid and early export of *Phaeocystis antarctica* blooms in the Ross Sea, Antarctica. Nature 404: 595–598

Dolan JR, Pierce RW, Yang EJ, Kim SY (2012) Southern Ocean biogeography of tintinnid ciliates of the marine plankton. J Eukaryot Microbiol 59:511–519

Dong S, Sprintall J, Gille ST, Talley L (2008) Southern Ocean mixed-layer depth from Argo float profiles. J Geophys Res Oceans 113:C06013

Dugdale RC, Wilkerson FP, Minas HJ (1995) The role of a silicate pump in driving new production. Deep-Sea Res I 42:697–719

Ebersbach F, Trull TW, Davies DM, Bray SG (2011) Controls on mesopelagic particle fluxes in the Sub-Antarctic and Polar Frontal Zones in the Southern Ocean south of Australia in summer — perspectives from free-drifting sediment traps. Deep-Sea Res II 58:2260–2276

Fripiat F (2011) Silicon pool dynamics and biogenic silica export in the Southern Ocean inferred from Si-isotopes. Ocean Sci 7:533–547

Hallegraeff GM, Bolch C, Hill D, Jameson I and others (2010) Algae of Australia, phytoplankton of temperate coastal waters. Australian Biological Resources Study, Canberra, and CSIRO Publishing, Melbourne

Herraiz-Borreguero L, Rintoul SR (2011) Regional circulation and its impact on upper ocean variability south of Tasmania. Deep-Sea Res II 58:2071–2081

Hillebrand H, Durselen CD, Kirschtel D, Pollingher U, Zohary T (1999) Biovolume calculation for pelagic and benthic microalgae. J Phycol 35:403–424

Iida T, Odate T (2014) Seasonal variability of phytoplankton biomass and composition in the major water masses of the Indian Ocean sector of the Southern Ocean. Polar Sci 8:283–297

Johnson R, Strutton PG, Wright SW, McMinn A, Meiners KM (2013) Three improved satellite chlorophyll algorithms for the Southern Ocean. J Geophys Res Oceans 118:3694–3703

Kirk JT (1994) Light and photosynthesis in aquatic ecosystems. Cambridge University Press, Cambridge

Klais R, Tamminen T, Kremp A, Spilling K, Olli K (2011) Decadal-scale changes of dinoflagellates and diatoms in the anomalous Baltic Sea spring bloom. PLOS ONE 6: e21567

Kopczynska EE, Savoye N, Dehairs F, Cardinal D, Elskens M (2007) Spring phytoplankton assemblages in the Southern Ocean between Australia and Antarctica. Polar Biol 31:77–88

Lannuzel D, Bowie AR, Remenyi T, Lam PJ and others (2011) Distributions of dissolved and particulate iron in the sub-Antarctic and Polar Frontal Southern Ocean (Australian sector). Deep-Sea Res II 58:2094–2112

Laurenceau-Cornec EC, Trull TW, Davies DM, De La Rocha CL, Blain S (2015) Phytoplankton morphology controls on marine snow sinking velocity. Mar Ecol Prog Ser 520: 35–56

Laws EA (2004) New production in the equatorial Pacific: a comparison of field data with estimates derived from empirical and theoretical models. Deep-Sea Res I 51: 205–211

Leblanc K, Hutchins DA (2005) New applications of a biogenic silica deposition fluorophore in the study of oceanic diatoms. Limnol Oceanogr Methods 3:462–476

Leblanc K, Arístegui J, Armand L, Assmy P, and others (2012) A global diatom database — abundance, biovolume and biomass in the world ocean. Earth Syst Sci Data Disc 5:147

Legendre L, Le Fevre J (1995) Microbial food webs and the export of biogenic carbon in oceans. Aquat Microb Ecol 9:69–77

Lourey MJ, Trull TW (2001) Seasonal nutrient depletion and carbon export in the Subantarctic and Polar Frontal zones of the Southern Ocean south of Australia. J Geophys Res Oceans 106:31463

MacIntyre HL, Kana TM, Anning T, Geider RJ (2002) Photoacclimation of photosynthesis irradiance response curves and photosynthetic pigments in microalgae and cyanobacteria1. J Phycol 38:17–38

Maldonado MT, Boyd PW, Abraham E, Bowie A and others (2001) Iron uptake and physiological response of phytoplankton during a mesoscale Southern Ocean Iron enrichment. Limnol Oceanogr 46:1802–1808

Marchetti A, Cassar N (2009) Diatom elemental and morphological changes in response to iron limitation: a brief review with potential paleoceanographic applications. Geobiology 7:419–431

Margalef R (1978) Life-forms of phytoplankton as survival alternatives in an unstable environment. Oceanol Acta 1: 493–509

Mariani P, Andersen KH, Visser AW, Barton AD, Kiørboe T (2013) Control of plankton seasonal succession by adaptive grazing. Limnol Oceanogr 58:173–184

Martin JH (1990) Glacial-interglacial CO_2 change: the iron hypothesis. Paleoceanography 5:1–13

Matear R, Hirst AC (1999) Climate change feedback on the future oceanic CO_2 uptake. Tellus 51:722–733

Matear R, Hirst AC, McNeil BI (2000) Changes in dissolved oxygen in the Southern Ocean with climate change. Geochem Geophys Geosyst 1:1050

Menden-Deuer S, Lessard EJ, Satterberg J (2001) Effect of preservation on dinoflagellate and diatom cell volume and consequences for carbon biomass predictions. Mar Ecol Prog Ser 222:41–50

Morel FMM, Reuter JG, Price NM (1991) Iron nutrition of phytoplankton and its possible importance in the ecology of ocean regions with high nutrient and low biomass. Oceanography 4:56–61

Norberg J (2004) Biodiversity and ecosystem functioning: a complex adaptive systems approach. Limnol Oceanogr 49:1269–1277

Paasche E (1973) Silicon and the ecology of marine plankton diatoms. I. *Thalassiosira pseudonana* (*Cyclotella nana*) grown in a chemostat with silicate as limiting nutrient. Mar Biol 19:117–126

Pender L, Trull TW, McLaughlin D, Lynch T (2010) Pulse-A mooring for mixed layer measurements in the open ocean and extreme weather. OCEANS 2010 IEEE, Sydney

Petz W (1999) Ciliophora. In: Boltovskoy D (ed) South Atlantic zooplankton. Backhuys Publishers, Leiden, p 265–319

Petz W (2005) Ciliates. In: Scott FJ, Marchant HJ (eds) Antarctic marine protists. Australian Biological Resources Study, Canberra, and Australian Antarctic Division, Hobart, p 347–448

Poloczanska ES, Burrows MT, Brown CJ, García Molinos J, and others (2016) Responses of marine organisms to climate change across oceans. Front Mar Sci 3:62

Queguiner B (2001) Biogenic silica production in the Australian sector of the Subantarctic Zone of the Southern Ocean in late summer 1998. J Geophys Res 106: 31627–31636

Queguiner B (2013) Iron fertilization and the structure of planktonic communities in high nutrient regions of the Southern Ocean. Deep-Sea Res II 90:43–54

Ragueneau O, Schultes S, Bidle K, Claquin P, Moriceau B (2006) Si and C interactions in the world ocean: importance of ecological processes and implications for the role of diatoms in the biological pump. Global Biogeochem Cycles 20:GB4S02

Rigual-Hernandez AS, Trull TW, Bray SG, Cortina A, Armand LK (2015) Latitudinal and temporal distributions of diatom populations in the pelagic waters of the Subantarctic and Polar Frontal zones of the Southern Ocean and their role in the biological pump. Biogeosciences 12: 5309–5337

Rintoul SR, Bullister JL (1999) A late winter hydrographic section from Tasmania to Antarctica. Deep-Sea Res I 46: 1417–1454

Rintoul SR, Trull TW (2001) Seasonal evolution of the mixed layer in the Subantarctic zone south of Australia. J Geophys Res Oceans 106:31447

Rintoul SR, Donguy JR, Roemmich DH (1997) Seasonal evolution of upper ocean thermal structure between Tasmania and Antarctica. Deep-Sea Res I 44:1185–1202

Roesler C, Uitz J, Claustre H, Boss E and others (2017) Recommendations for obtaining unbiased chlorophyll estimates from in situ chlorophyll fluorometers: a global analysis of WET Labs ECO sensors. Limnol Oceanogr Methods 15:572–585

Sabine CL, Feely RA, Gruber N, Key RM and others (2004) The oceanic sink for anthropogenic CO_2. Science 305: 367–371

Sarmiento JL, Le Quéré C (1996) Oceanic carbon dioxide uptake in a model of century-scale global warming. Science 274:1346–1350

Sarmiento JL, Gruber N, Brzezinski MA, Dunne JP (2004) High-latitude controls of thermocline nutrients and low latitude biological productivity. Nature 427:56–60

Schoemann V, Becquevort S, Stefels J, Rousseau V, Lancelot

C (2005) *Phaeocystis* blooms in the global ocean. J Sea Res 53:43–66

Scott F, Marchant HJ (2005) Antarctic marine protists. Australian Biological Resources Study, Canberra, and Australian Antarctic Division, Hobart

Sedwick PN, DiTullio GR, Hutchins DA, Boyd PW and others (1999) Limitation of algal growth by iron deficiency in the Australian Subantarctic region. Geophys Res Lett 26: 2865–2868

Sedwick PN, Bowie AR, Trull TW (2008) Dissolved iron in the Australian sector of the Southern Ocean (CLIVAR SR3 section): meridional and seasonal trends. Deep-Sea Res I 55:911–925

Shadwick EH, Trull TW, Tilbrook B, Sutton AJ, Sabine CL, Schulz E (2015) Seasonality of biological and physical controls on surface ocean CO_2 from hourly observations at the Southern Ocean Time Series site south of Australia. Global Biogeochem Cycles 29:223–238

Sigman DM, Boyle EA (2000) Glacial/Interglacial variations in atmospheric carbon dioxide. Nature 407:859–869

Sokolov S, Rintoul SR (2002) Structure of Southern Ocean fronts at 140° E. J Mar Syst 37:151–184

Sournia A (1978) Phytoplankton manual. UNESCO Monogr Oceanogr Methodol 6. UNESCO, Paris

Strom SL, Wolfe GV, Holmes JL, Stecher HA, Shimeneck C, Lambert S, Moreno E (2003) Chemical defense in the microplankton I: Feeding and growth rates of heterotrophic protists on the DMS-producing phytoplankter *Emiliania huxleyi*. Limnol Oceanogr 48:217–229

Strzepek RF, Hunter KA, Frew RD, Harrison PJ, Boyd PW (2012) Iron–light interactions differ in Southern Ocean phytoplankton. Limnol Oceanogr 57:1182–1200

Sugie L, Kuma K (2008) Resting spore formation in the marine diatom *Thalassiosira nordenskioeldii* under iron- and nitrogen limited conditions. J Plankton Res 30:1245–1255

Sverdrup HU (1953) On the conditions for the vernal blooming of phytoplankton. ICES J 18:287–295

Takao S, Hirawake T, Hashida G, Sasaki H, Hattori H, Suzuki K (2014) Phytoplankton community composition and photosynthetic physiology in the Australian sector of the Southern Ocean during the austral summer of 2010/2011. Polar Biol 37:1563–1578

Takeda S (1998) Influence of iron availability on nutrient consumption ratio of diatoms in oceanic waters. Nature 393:774–777

Tang KW (2003) Grazing and colony size development in *Phaeocystis globosa* (Prymnesiophyceae): the role of a chemical signal. J Plankton Res 25:831–842

Thomas WH, Vernet M, Gibson CH (1995) Effects of small-scale turbulence on photosynthesis, pigmentation, cell division, and cell size in the marine dinoflagellate *Gonyaulax polyedra* (Dinophyceae). J Phycol 31:50–59

Thomas MK, Kremer CT, Litchman E (2016) Environment and evolutionary history determine the global biogeography of phytoplankton temperature traits. Glob Ecol Biogeogr 25:75–86

Thompson GA, Alder VA, Boltovskoy D, Brandini F (1999) Abundance and biogeography of tintinnids (Ciliophora) and associated microzooplankton in the Southwestern Atlantic Ocean. J Plankton Res 21:1265–1298

Tomas C (1997) Identifying marine phytoplankton. Academic Press, San Diego, CA

Trull TW, Bray SG, Manganini SJ, Honjo S, Francois R (2001a) Moored sediment trap measurements of carbon export in the Subantarctic and Polar Frontal Zones of the Southern Ocean, south of Australia. J Geophys Res Oceans 106:31489–31509

Trull TW, Rintoul SR, Hadfield M, Abraham ER (2001b) Circulation and seasonal evolution of polar waters south of Australia: implications for iron fertilization of the Southern Ocean. Deep-Sea Res II 48:2439–2466

Trull TW, Sedwick PN, Griffiths FB, Rintoul SR (2001c) Introduction to special section: SAZ Project. J Geophys Res Oceans 106:31425–31429

Trull TW, Schulz E, Pender L, McLaughlin D, Tilbrook B, Rosenberg R, Lynch T (2010) The Australian Integrated Marine Observing System Southern Ocean Time Series. IEEE OCEANS 2010, Sydney

Trull TW, Passmore A, Davies DM, Smit T, Berry K, Tilbrook B (2018) The distribution of pelagic biogenic carbonates in the Southern Ocean south of Australia: a baseline for ocean acidification impact assessment. Biogeosciences 15:31–49

Turner JT (2015) Zooplankton fecal pellets, marine snow, phytodetritus and the ocean's biological pump. Prog Oceanogr 130:205–248

Wang XJ, Matear RJ, Trull TW (2001) Modeling seasonal phosphate export and resupply in the Subantarctic and Polar Frontal Zones in the Australian sector of the Southern Ocean. J Geophys Res Oceans 106:31525–31541

Weeding B, Trull TW (2014) Hourly oxygen and total gas tension measurements at the Southern Ocean Time Series site reveal winter ventilation and spring net community production. J Geophys Res Oceans 119: 348–358

Westwood KJ, Griffiths FB, Webb JP, Wright SW (2011) Primary production in the Sub-Antarctic and Polar Frontal zones south of Tasmania, Australia; SAZ-Sense survey, 2007. Deep-Sea Res II 58:2162–2178

Wright SW, van den Enden RL, Pearce I, Davidson AT, Scott FJ, Westwood KJ (2010) Phytoplankton community structure and stocks in the Southern Ocean (30–80° E) determined by CHEMTAX analysis of HPLC pigment signatures. Deep-Sea Res II 57:758–778

Editorial responsibility: Antonio Bode, A Coruña, Spain

Submitted: December 16, 2016; Accepted: November 20, 2017
Proofs received from author(s): February 19, 2018